International Conference on Space Optics—ICSO 2022

Dubrovnik, Croatia

3–7 October 2022

Edited by Kyriaki Minoglou, Nikos Karafolas, and Bruno Cugny,

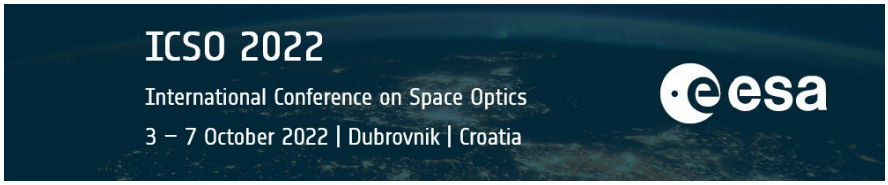

Laser Beam Soldering of exotic optic materials

International Conference on Space Optics — ICSO 2022, edited by Kyriaki Minoglou, Nikos Karafolas, Bruno Cugny, Proc. of SPIE Vol. 12777, 127777G · © 2023 ESA and CNES · 0277-786X · doi: 10.1117/12.2691443

Laser Beam Soldering of exotic optic materials

G. Rosario Rodriguez*[a, b], E. Beckert[a], M. Hornaff[a,c], T. Peschel[a], T. Schmidt[a], M. Heimberg[a]
[a] Fraunhofer Institute for Applied Optics and Precision Engineering IOF, Albert-Einstein-Str. 7, 07745 Jena, Germany
[b] Friedrich-Schiller-University Jena, Institute for Applied Physics, Abbe Center of Photonics, Jena, Germany
[c] The author is now with SpaceOptix GmbH, Hans-Knöll-Straße 6, 07745 Jena, Germany
*Correspondence: Grucheska.rosario.rodriguez@iof.fraunhofer.de; +49 3641 807-574

ABSTRACT

Low-stress bonding using the laser-based soldering technique Solderjet Bumping is presented for the assembly of optical systems. Selected systems include SQ1 and INVAR 36 (baseline system), CaF2 and 1.4371 stainless steel, BBO and Dilver P1, and KTP and Super Invar, the first two proposed as lens demonstrators and the other two as laser crystal demonstrators. Solder parameters found for the SQ1 and INVAR using the DoE method using 400µm SAC305 alloy with the desirability of 0.655, for BBO and Dilver P1 and CaF2 and stainless steel 1.4371 systems, parameters must be changed due to damage observed in the optical components. KTP and Super Invar system parameters are still under investigation. In the case of BBO, the parameters were successfully found while CaF2 is still under investigation, changing the solder bump size due to the constant presence of damage in the samples. Finite elements simulations show that excessive stress occurs locally at the singularity of the soldered interface, but is still below the critical value, nevertheless, the survival of the demonstrators under environmental loads (Δ60 K, 600 g) is expected.

Keywords: Solderjet bumping, Laser soldering, adhesive-free, optic materials, optics systems assembly

1. INTRODUCTION

Space optics, in particular active optics systems such as laser sources, objectives for both imaging and illuminating processes, and lens assembly groups, contain a wide variability of materials with very specific properties, such as coefficient of thermal expansion (CTE), thermal conductivity, anisotropy, brittleness and softness, sensitivity to contamination, and birefringence sensitivity to mechanical stress. Furthermore, such systems must withstand high environmental conditions (e.g., mechanical and thermal loads, contamination, radiation) during their lifetime while ensuring optimum performance (especially optical alignment stability). Most optical components such as lenses, mirrors, fibers, and gratings, are typically assembled on tools made of different materials such as metal, glass, and ceramics, providing the system with more variable mechanical properties. [1, 2]

The assembly of these hybrid systems is the last step in the optics component manufacturing chain. And besides alignment, it is one of the most critical process steps, as its main goal is to fix and ensure the previously achieved alignment state, taking into account the lifetime of the components and expected operating and non-operating conditions such as mechanical and thermal changes in the environment. Therefore, finding a bonding technology that solves most, if not all, of the potential problems caused during this step could lead to a technology that can be used for the vast majority of optical applications, not only in space but also in generally hostile environments. [2]

Solderjet Bumping (SJB) is a laser-based, flux-free technology for joining optical components, using spherical preforms of various high-melting and low-melting soft solder alloys ranging from 40 µm to 760 µm in diameter, that are reflowed by a laser and then applied in a liquid state to a wettable surface to form an intermetallic phase or mixed crystals (depending on the solder alloy used and phases used) to form the connection, the process scheme can be observed in figure 1. This technique in general applies a low and localized thermal impact during soldering and is well suited for heterogeneous material combinations with different CTE or thermal conductivities. Previous to the soldering step, it must be ensured that both surfaces are wettable, which can be done by metallization processes that can be applied by different techniques, such as physical vapor deposition (PVD) or screen printing. [3]

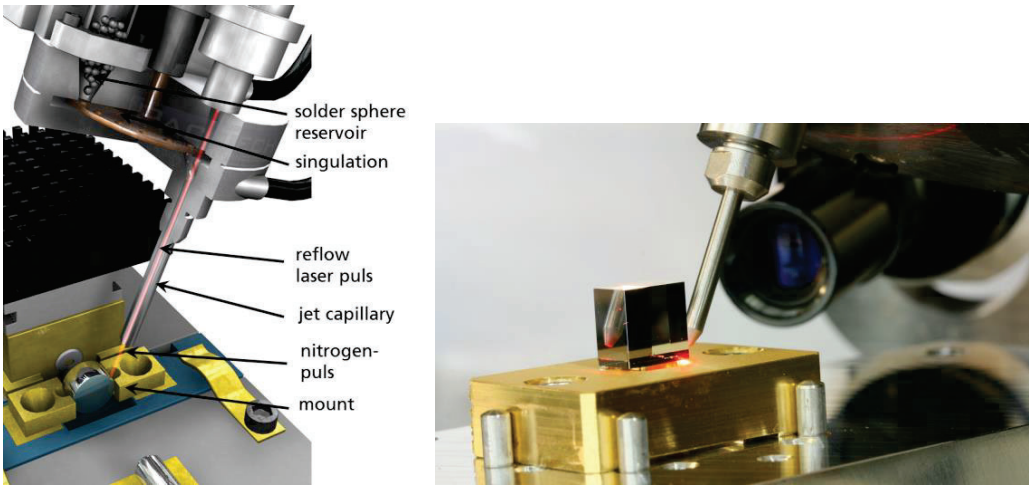

Figure 1. (Left) Solderjet-bumping process schema and (right) during the soldering of a mirror. [1]

As shown in figure 1, the capillary is guided by a pilot laser with respect to the position where solder bumps are to be placed. Based on a mechanical singulation system, the spherical solder preform goes out of the reservoir by gravitational forces to the capillary, which is slightly smaller than the sphere size. Then, both the laser pulse and nitrogen gas pressure are applied, pushing the melted solder bump out of the capillary to the desired position, allowing the joining of complex geometries. This technology has been previously investigated and used as the primary assembly technique in several other projects, some examples are shown in figure 2, such as the precise assembly of large lenses in frames, the construction of a miniaturized green laser for the EXOMARS Raman experiments, and the assembly of a multi-beam deflection array for lithography, to name a few. This is due to its several advantages including sub-micron precision in components placement with six degrees of freedom, vacuum compatibility due to the absence of organic components, and the ability to bond dissimilar materials. [1-8]

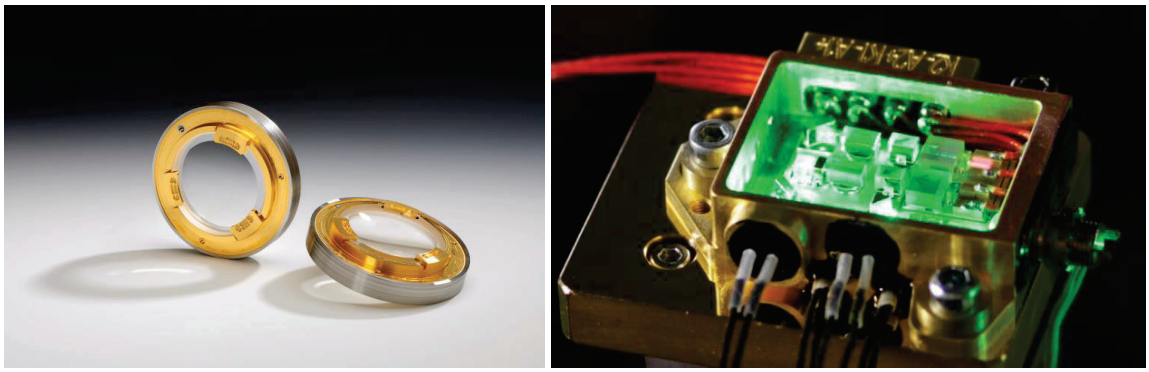

Figure 2. (Left) Large lens mount soldered with SJB and (right) assembled miniaturized green laser device. [6, 8]

The different materials used in optics depend on their properties and ability to manipulate light, and their selection is based on the details of optical design and instrument functionality. We define as “exotic material” those with different required properties in the laser field, where both performance and environment conditions are of great importance. These materials vary widely, some of them can be classified into different categories depending on their application: UV grade i.e., materials that have good performance (such as transmission) in the UV spectrum and can be used as visible optics (including SQ1, SF6, LAK9, MK7), radiation resistant materials commonly used in free electron lasers, e.g., BK7G18, LF5G19, LAK9G15, materials that act as active mediums like YAG, Al2O3, YVO4, and non-linear crystals such as CaF2. BaF2, BBO. KTP, MgF2. [9, 10]

The challenge is to be able to join the optical materials (predominantly, crystals and glasses, and thus rather brittle materials, presumably) with the mount materials that are usually metals or ceramics. Stresses can already be induced by environmental conditions, especially thermal loads due to the expansion of the different materials, so the CTE of the mount material should be as close as the CTE of the optics to minimize these effects. [2]

The selection of a series of material combinations of optics and mount materials with low CTE mismatch as the principal requirement and hybrid systems that could be used later on without major redesign. Followed by the selection of soft-solder bonding media materials, and laser process parametrization based on Design-of-Experiment (DoE) parameter variation was part of the first approach to technology selection. This was followed then by a CAD and finite element method (FEM) based analysis of demonstrator designs vs. environmental loads, leading to an optimization of laser process parameters based on the previous Design-of-Experiment parameter results. This process will be explained more in detail in the following sections.

2. MATERIALS AND PROCEDURES

2.1 Materials selection

The choice of materials used takes into account the requirements imposed by a spacecraft's flight unit, where no major redesign is required, e.g., flammability, outgassing, and susceptibility to stress corrosion. First, the selection of baseline materials was conducted to prove the feasibility of the soldering process. Fused Silica (SQ1) is used as the optical material which is commonly used for lenses, and the mounting material is Invar 36. Then, due to their importance in laser resonators, CaF2, BBO, and KTP, all non-linear crystal materials were selected for the evaluation. The table below compares various lens and frame material combinations, and the properties considered when selecting.

Table 1. Physical properties of optical and mounting materials, including their best combinations.

Optical Material			Mount Material			Material Combination
	CTE 20/300 [10-6/K]	Thermal Conductivity [W/mK]		CTE 20/300 [10-6/K]	Thermal Conductivity [W/mK]	Delta CTE [10-6/K]
SQ1	0,55	1,31	INVAR 36	1,26	14	-0,71
KTP	0,60	3,30	Super Invar	0,63	10	-0,03
BBO	4	0,08	Dilver P1	4,6	17,5	-0,6
CaF2	21,28	9,71	Stainless steel 1.4371	20,2	138	-1.08

Table 1 shows the CTE and also the thermal conductivity of all selected materials, as the mount material offers higher thermal conductivity values, solderability, and thermal connections are limited by the optical material. But as mentioned, the main requirement for material selection is a low delta CTE to reduce stress over the temperature range conditions.

The choice of solder alloy and size is also very important, since the SJB energy applied to melt also determines the thermal impact and effect of the soldering on the surface. The eutectic ternary alloy 96,5Sn-3,5Ag-0,9Cu SAC305 was chosen as the reference starting solder, it has a lower melting point (around 217°C), compared to other commonly used solders such as AuSn alloys and therefore can be processed at a lower temperature, reducing the possibility of damage due to heat exposure.

2.2 Solder Jet Bumping

Previous to the application of the Solderjet bumping, samples optics and mounting materials must be prepared. To ensure adequate wetting of the solder bumps to the material surface, they should be previously metalized. All materials were first cleaned, for fused silica, a thorough ultrasonic-assisted solution followed by rinsing in high-purity water was used, and for the non-linear crystals, a manual cleaning process with acetone was done. A three-layer system metallization composed of Titanium, platinum, and gold (Ti/Pt/Au) with a thickness of around 0,5 µm was then applied on the surfaces of all materials, using DC magnetron sputtering (MRC2, Material Research Corp., USA) in a single run. To

ensure good adhesion strength, witness samples were tested according to the corresponding procedure (DIN EN ISO 2409). The PacTech SB2-Automatic equipped with a fiber-coupled 100 W laser source Solderjet bumper was used for processing all samples.

The solder parametrization process started with the baseline materials (SQ1 and INVAR 36), as this has been already parametrized in previous projects.[2] Nevertheless, to optimize these parameters, the laser pulse energy was first measured as a starting point to assure a proper wetting of both materials and melting of the bump, and also prevent any damage induced on the fragile materials. Laser current and laser pulse width are the main two parameters on which the energy depends and the two which will be changed during the parametrization. Due to the different thermal conductivities and CTE of the optics and mount materials, it is challenging to find an acceptable trade-off manually, therefore the methods of design of experiment (DoE) are used to investigate the different responses from the single parameters.

An overall scope of 30 runs was the initial target, changing in between the laser current and laser pulse width while maintaining the rest of the parameters. Applied bumps on both crystals, glasses, and metals were then visually inspected using a Keyence VHX6000 Visual Microscope, where bumps' diameter was measured and damage on the optical samples was observed and measured as well. Afterward, shear forces were measured using a Delvotec Bonder 5630 (incl. shear module SH5000) shear tester. From this data, a DoE was created and used to select the optimum parameters for each combination, which will be ultimately used in the demonstrator assembly phase.

2.3 Demonstrator requirements

The systems to be built with the SJB technique have to meet the following target performance requirements:

- Solder bonding accuracy: optical and alignment performance before, during, and after the process chain with expected results to be <5 µrad dealignment in tip/tilt, <10 nm birefringence change in the optical aperture, <20 nm P-V wavefront change in total.
- Meet minimum displacement requirements before and after thermal cycling: 10 thermal cycles conducted from -40° C to +50° C non-operational, expected results to be <20 µrad dealignment.
- Meet minimum displacement requirements before and after vibration test: 5 min of random vibration (20 Hz – 2000 Hz at 1 g 2/Hz along the worst axis) and shock (survival shock 3x per direction per axis (18 shocks in total) to an SRS higher than the SRS of a 600 g 0.5 ms half-sine impulse) testing. Expected results to be <5 µrad dealignment in tip/tilt, <10 nm birefringence change in the optical aperture, and <20 nm P-V wavefront change.
- Demonstrators' design for both lens barrel and optical bench should be as simple as possible to minimize extra induced stresses due to thermal cycling or mechanical loads. It has to be taken into consideration the soldering tool and how it will be applied to the system to assembly.

2.4 Characterization of demonstrators

One of the main requirements is to ensure the long-term stability of the alignment. To evaluate and assess the results, position accuracy will be measured before, during, and after the soldering process, and then before and after the environmental cycling, including thermal and mechanical variations. The following characterization techniques will be conducted in order to assess the results:

- Autocollimation telescope measurement of tip and tilt alignment of the optical component vs. mount.
- 3D coordinate measurement for 5-6 Degrees of Freedom alignment of the optical component vs. mount.
- Interferometer measurement of the components' P-V.
- Polarimeter measurement of the components' birefringence.

3. RESULTS

3.1 FEM Analysis

The FEM analysis of the lens demonstrator examined two different material combinations: A lens made of CaF2 in a mount made of stainless steel 1.4371, and a lens made of Fused Silica (SQ1) in an Invar mount, the crystal deformation was analyzed by means of BBO as optical material in combination with Dilver P1 as the mount material. A few assumptions were initially made on these models: simplification of the solder joint geometry, the threads in screw holes, and fiducials removed. Using the ANSYS 2020.1 classic analysis code and assuming linear material properties, a structural analysis of the assembled demonstrators was investigated for: acceleration, temperature, and eigenfrequencies changes, figure 6 shows the first results for the eigenfrequencies deformations.

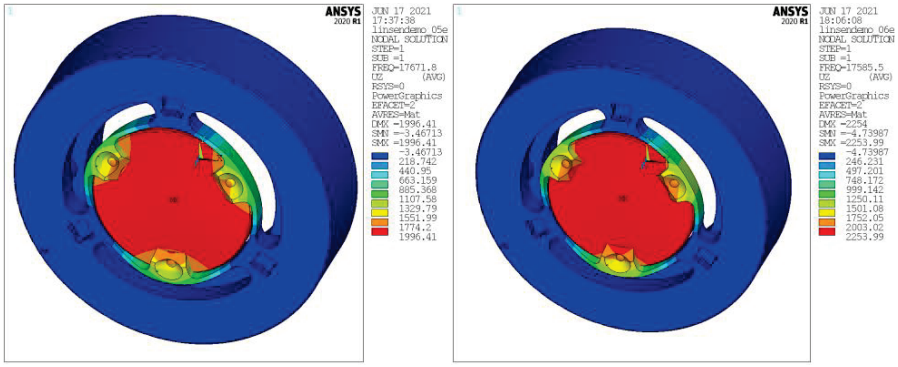

Figure 3. Shapes of the Eigenmodes of the lens demonstrators in the axial direction (z), (left) the CaF2 system, (right) the SQ1 system.

First, a model check of the simulation revealed no significant displacement or stress, and eigenfrequencies of the rigid body of <0.02 Hz. Modal analysis of the lens mount demonstrators shows a fundamental frequency of 17.7 kHz for the CaF2 and 17.6 kHz for the SQ1 system. In both cases, the results were well above the required value of 2 kHz. Vibration and shock stimuli typically have frequencies below this value, so the lens response to a 133.5 g vibration stimulus (corresponding to 3 σ r.m.s value) and a 600 g shock load is considered quasi-static. Figure 7 shows the lowest eigenmode of the lens demonstrator with the largest displacement in the axial z-direction.

For the case of the crystal demonstrator, the eigenfrequencies of the rigid body mode are <0.03 Hz. The model analysis yields a fundamental frequency of 1.44 kHz, this result can be considered quasi-static as it is below the requirement of the first Eigenfrequency above 2 kHz. However, this mode can be characterized as the crystal rotates around x (as shown on the left in figure 8), so the effective mass of this mode is negligible relative to linear vibrations. Therefore, the vibration response is driven by higher modes starting at 4.1 kHz, and figure 8 (right) shows the shift in axial x in mode #3, which in this case is the largest component of the shift.

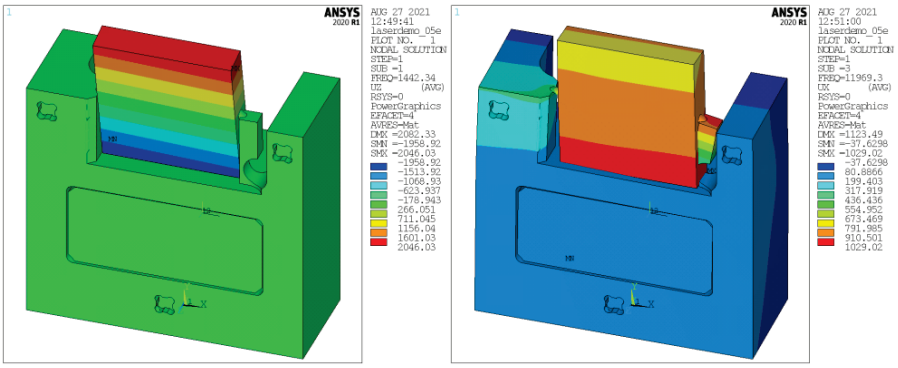

Figure 4. Shapes of the lowest Eigenmodes of the crystal demonstrator. Displacement in z (left) for mode #1 and in x (right) for mode #3.

Under a change in ambient temperature by 10 K the lens demonstrator deforms as shown in figure 9, it can be observed as this is dominated by the effect of thermal expansion. The corresponding surface deformation of the optical element is shown in Figure 10 dominated by a defocus term. The peak-to-valley deformation in the quality area under maximum operational temperature (ΔT=20K) will reach 24 nm in the case of CaF2 and 8 nm in the case of SQ1.

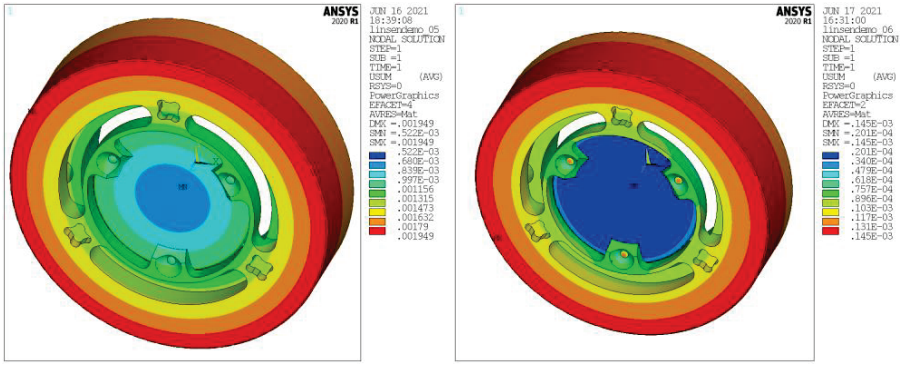

Figure 5. Deformation (absolute value in mm) of the lens dummies due to a change in ambient temperature by 10 K, (left) CaF2 system, and (right) SQ1.

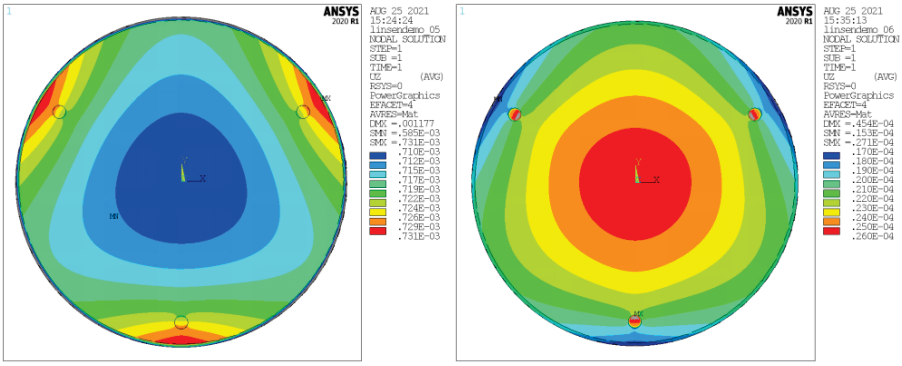

Figure 6. Surface deformation (absolute value in mm) of the lens dummies due to a change in ambient temperature by 10 K, (left) CaF2 system, and (right) SQ1.

In the worst-case scenario, the systems were under a Δ60K change at -40 °C, results are listed in table 2 below.

Table 2. Maximum stress in the optical components of the lens demonstrators under an ambient temperature of -40 °C.

Component	Maximum stress at -40 °C [MPa]		
	CaF2	SQ1	BBO
Optical element	28.3	48.6	48
Mount ring	228	628	237
Solder	28.6	106.7	109

In the SQ1 system, localized stresses exceed the material limits for the invar mount, these large single-element values are positioned at the inner line in contact with the solder, forming a singularity, the same could also be explained for the BBO soldering result. These values are considered exaggerated and could be compared with those shown in table 3, nevertheless, the solder must be analyzed in more detail.

Table 3. Materials tensile strength.

Material Component	CaF2	SQ1	BBO	Steel 1.4371	Invar	Kovar	SAC305
Tensile Strength [MPa]	157	80	13	650	276	517	35

The ultimate strength given in Table 3 is from the shear test of the solder bump. Therefore, this value represents the "technical" stress averaged over the specimen area and cannot represent the local maxima that can also be found in the test geometry.

In this simulation, we found a shear force of 0.17 N per solder joint (0.4 mm diameter) for CaF2, 0.055 N for SQ1, and 0,05 N for BBO (0,2263 mm^2 of contact area). Scaling these values to 60 K, the resulting "technical" stress in the solder reaches 8.1 MPa for CaF2, 2.7 MPa for silica, and 0,13 MPa for the BBO system which is well below the limit of the solder material.

For the BBO crystal demonstrator shown in figure 11 (left), the behavior is similar to the lens demonstrator, dominated by the effect of thermal expansion. The surface deformation is dominated by local effects close to the solder points and it can be observed in figure 11 (right). The peak-to-valley deformation in the quality area under maximum operational temperature (ΔT=20K) will reach appr. 6 nm.

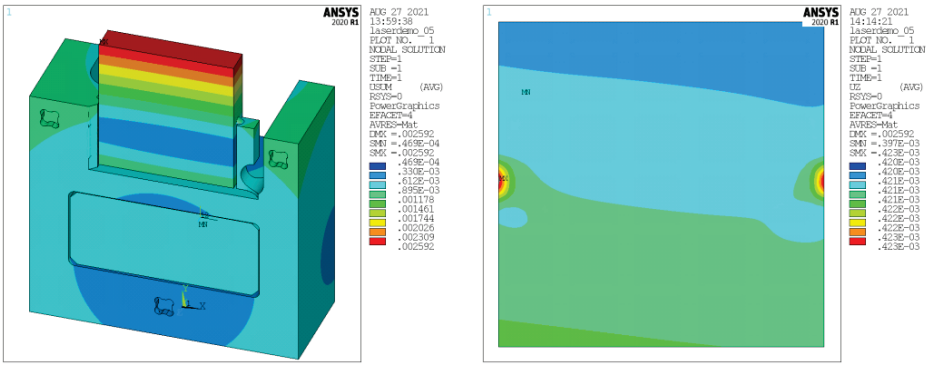

Figure 7. Deformation (absolute value in mm) of the laser crystal demonstrator due to a change in ambient temperature by 10 K, (left) BBO system, (right) surface deformation.

Accelerations of 1 g in the different axis were applied, to get the results of the stress distributions of the demonstrators. For all the directions, even in the worst case, where there's an acceleration of 600 g which corresponds to the maximum expected shock load, all the values stay well below the strength of the respective materials as shown in table 3.

Table 4. Maximum stress [MPa] in the components of the lens demonstrator under acceleration with 600 g.

	Maximum stress at 600 g					
Component	In x [MPa]		In y [MPa]		In z [MPa]	
	CaF2	SQ1	CaF2	SQ1	CaF2	SQ1
Optical element	15.1	11.6	15.9	12.1	6.78	4.75
Mount ring	94.8	68.4	93.6	66	109	67.8
Solder	19.7	15.3	19.7	15	9.66	6.6

A similar approach was applied to the crystal demonstrator, results are shown in Table 4.

Table 5. The maximum stress in the components of the crystal demonstrator under acceleration with 600 g.

	Maximum stress at 600 g		
Component	In x [Mpa]	In y [MPa]	In z [MPa]
Optical element	52.1	35.3	**92**
Mount	406	226	**551**
Solder	**266**	**82.8**	**334**

In this case, we can observe the highlighted values, which means that the maximum local stress exceeds the material limit, these large values are located in individual elements at the solder boundary line, forming singularities, similar to the -40 °C case it can be considered as an exaggeration, as shown in figure 12.

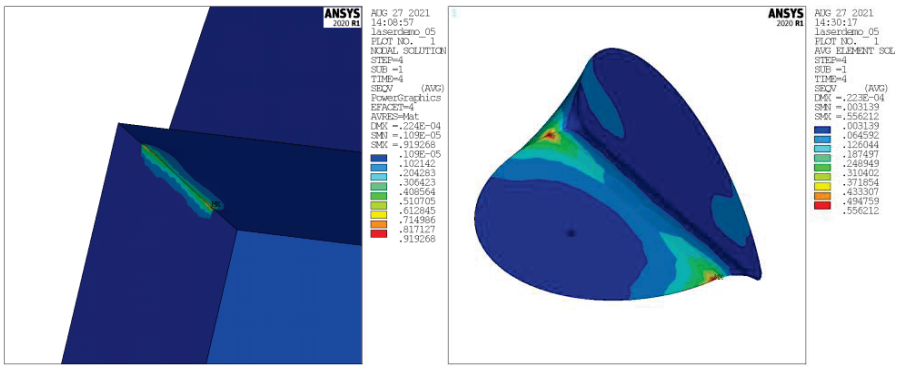

Figure 8. Distribution of equivalent stress (v. Mises in MPa) in the metal components of the laser crystal demonstrator under acceleration with 1 g in the z-direction, (left) mount component and (right) solder alloy.

In the simulation, it is found maximum shear forces of 0.399E-2 N at the solder joints (contact area: 0.2263 mm²). Scaling these values to an acceleration of 600 g the resulting "engineering" stress in the solder will reach 10.6 MPa, which is below the limit for the solder material.

3.2 Design of Experiments

For demonstrator assembly, the SAC305 400 µm soldering parameters needed to be selected and optimized, to ensure good wetting of the two components (optics and mount) while preventing any induced damage to the optics and

maximizing bond strength. As described in section 2.2, SQ1 was used as baseline material. Table 5 shows the parameters chosen from the design of the experiment for each combination.

Table 6. Laser parameters obtained by DoE.

Optical Material	Mount Material	Laser Current [mA]	Laser Pulse Width [ms]	Desirability	Shear Strength [MPa]
SQ1	INVAR 36	8000	0,1	0.655	0,06

To obtain these results from the DoE, bump wetting and shear values are maximized on both the optic and mount material while minimizing damage to the optical material. Desirability represents an optimization of all of these values, with values close to 1 indicating that almost all limits have been reached, while lower values indicate a compromise between various parameters, wetting, and damage.

However, after obtaining the DoE parameters, verification was done from where it was observed that some parameters were damaging the optical materials, this was observed on BBO and CaF2 samples as shown in figure 3, two materials that are characterized by their brittleness. A second optimization was proposed in order to diminish these damages.

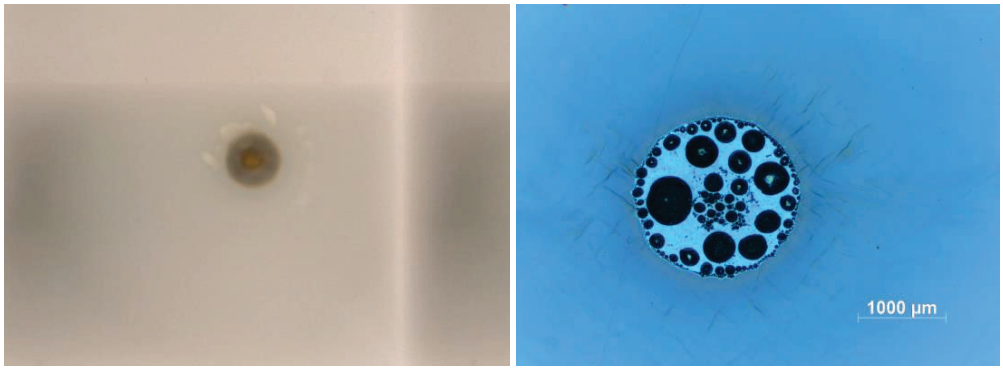

Figure 9. Damages observed in BBO (left) and CaF2 (right) crystals with parameters proposed by the DoE.

The first step is to reduce the laser pulse energy for both materials. The laser pulse energy cannot be too low as it wouldn't be possible for solder bumps to melt and wet the surface, assuring that the laser energy is still high enough to melt the bumps but not too low to damage the BBO surface, also the other restrictions were once again measured in order to no compromise both the surface wetting and shear strength.

In the case of CaF2, the total energy of the laser pulse is too high for the material, and the damage occurs not only where the laser pulse is applied but also cracks form around the bumps. The process is similar to that applied on BBO, but in this case, both parameters are initially reduced at the same time. Figure 4 shows the different parameters proposed for the soldering of CaF2. It must be taken into account that the CaF2 structures have different orientations and different damages can be observed depending on this factor.

Figure 10. Soldering parametrization of CaF2, damage was observed with different parameters used.

Due to the high recurrence of damage observed with the 400 µm bump size, a change of parameters and bump size was proposed for CaF2, to solder an array with 150 µm bumps and then solder larger bumps on top. This method has been already used in other projects [6] in order to protect bulk materials from the impact made by the larger solder spheres. Although no material damage was observed at a single bump, damage can still be observed on the surface where the array and larger bumps were applied in figure 5.

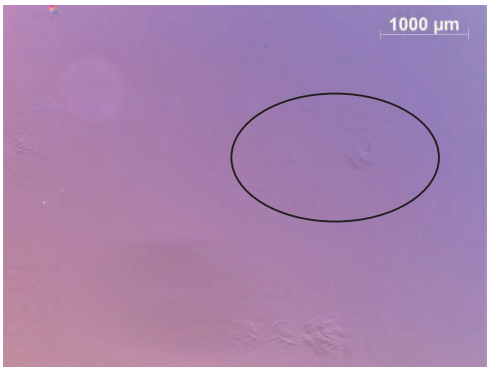

Figure 11. Soldering of a 150µm array with different parameters (4000mA, 0,5ms)

Due to the lack of material availability (super invar) in-house, the KTP-Super Invar combination has no desirability values available. Values for soldering without damaging the KTP sample (shown on the left in figure 6) have been already found, these should be tested next in the mount bulk material and analyzed for its selection. Although desirability values indicate whether all boundary conditions are met, it doesn't work in the case of CaF2. It could be due to the brittleness of the material and how the orientation of the material in these samples, a more in-depth investigation has to be done to find out new parameters. [10]

For the SQ1-Invar system the conditions were met, the bumps in SQ1 are shown on the right side of figure 6. The shear testing results for both SQ1 and BBO (with the parameters optimized, 5260 mA and 3,5 ms) are shown in table 7.

Table 7. Shear test values.

Material Component	SQ1	BBO
Maximum shear load [N]	11,85	11,62

Comparing these results with the simulated ones, much higher values than the simulated ones were obtained. However, it must be taken into account that these tests were performed on bulk material in not controlled conditions, future evaluations in demonstrator geometry and under controlled conditions will be performed to reevaluate these results.

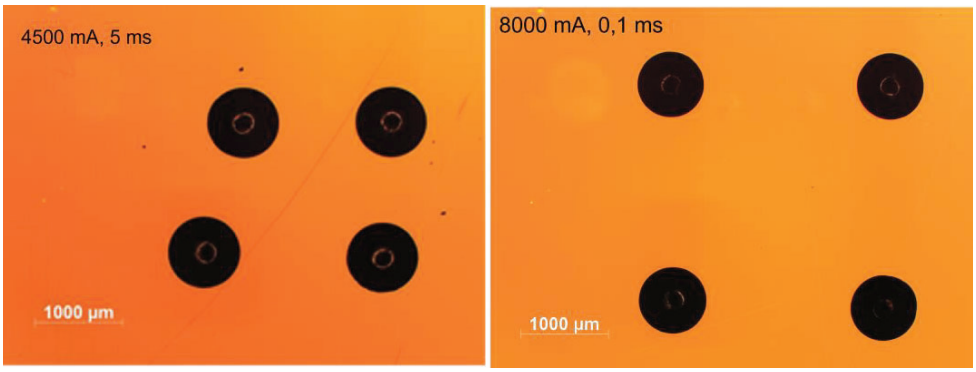

Figure 12. Verification of parameters obtained for (left) KTP and (right) SQ1.

4. CONCLUSIONS AND OUTLOOK

Parametrization of the lens and crystal demonstrators was done for two of the proposed systems. While KTP has still to be investigated with respect to the mount material (in both DoE and FEM simulation), CaF2 parametrization requires further examination to find new parameters for both the array and the larger bump on top. Furthermore, considering the crystal orientation, more in-depth studies are needed on how to reduce surface damage. The results of the finite element simulation showed that the demonstrators will survive the influence of the environmental loads. Excessive stresses occur locally at singular points of the solder interface, yet the total joint forces remain below critical values. The laser crystal demonstrator has a first eigenfrequency below 2 kHz, however, the respective effective masses are so small that the effect of this mode on the vibrational behavior is negligible.

As a final step, various lens and crystal demonstrators will be manufactured to measure optical (birefringence and P-V resolution) and alignment (tip/tilt) performance parameters before, during, and after the soldering process to be performed. Environmental testing as well as thermal and mechanical load cycles, where the optical and alignment parameters will be characterized to evaluate the performance of the assembled systems.

5. ACKNOWLEDGEMENTS

The authors would like to thank Technische Universität Wien (TU Vienna) for the collaboration on the first phase of the project.

REFERENCES

[1] P. Ribes Pleguezuelo, C. Koechlin, M. Hornaff, A. Kamm, E. Beckert, G. Fiault, R. Eberhardt, A. Tünnermann, “High-precision optomechanical lens system for space applications assembled by a local soldering technique,” Opt. Eng. 55(6), 065101 (2016), DOI:10.1117/1.OE.55.6.065101.

[2] T. Burkhardt, M. Hornaff, A. Kamm, D. Burkhardt, E. Schmidt, E. Beckert, R. Eberhardt, A. Tünnermann, “Low-Strain Laser-Based Solder Joining of Mounted Lenses.” Proc. SPIE 9574, Material Technologies and Applications to Optics, Structures, Components, and Sub-Systems II, 95740M (2 September 2015); DOI: 10.1117/12.2186747

[3] H. Banse, E. Beckert, R. Eberhardt, W. Stöckl, and J. Vogel, “Laser beam soldering – a new assembly technology for microoptical systems,” Microsyst. Technol., vol. 11, no. 2–3, pp. 186–193, Feb. 2005, DOI: 10.1007/s00542-004-0451-y.

[4] R. Eberhardt, E. Beckert, T. Burkhardt, S. Böhme, T. Schreiber, and A. Tünnermann, “Optoelectronic packaging based on laser joining,” San Jose, CA, Feb. 2008, p. 68800G. doi: 10.1117/12.763105.

[5] M. Hornaff, T. Burkhardt, A. Kamm, “Low-Stress Soldered Lenses for High-Perfomance Objectives - Fraunhofer IOF.” Fraunhofer Institute for Applied Optics and Precision Engineering IOF. https://www.iof.fraunhofer.de/en/business-fields/precision-engineering-components-and-systems/low-stress-soldered-lenses-for-high-perfomance-objectives.html

[6] P. Ribes Pleguezuelo, “Low-Stress soldering process to assemble highly stable and miniaturized laser resonators,” Friedrich-Schiller University of Jena, Germany, 2018
[7] E. Beckert, T. Oppert, G. Azdasht, E. Zakel, T. Burkhardt, M. Hornaff, A. Kamm, I. Scheidig, R. Eberhardt, A. Tünnermann, F.Buchmann, “Solder Jetting - A Versatile Packaging and Assembly Technology for Hybrid Photonics and Optoelectronical Systems,” IMAPS 42nd International Symposium on Microelectronics, Proceedings, 406-412 (2009).
[8] E. Beckert, T. Burkhardt, M. Hornaff, A. Kamm, I. Scheidig, C. Stiehl, R. Eberhardt, and A. Tünnermann "Submicron accuracy optimization for laser beam soldering processes", Proc. SPIE 7585, Laser-based Micro- and Nanopackaging and Assembly IV, 758505 (23 February 2010); DOI:10.1117/12.840495
[9] P. Sergeev, A. Sergeev, V. Zvorykin, “Radiation resistance of optical materials for windows of UV and VUV excimer lasers” (2007). Quantum Electronics - QUANTUM ELECTRON. 37. 706-710. DOI: 10.1070/QE2007v037n08ABEH013444.
[10] Collier, D., Schuster, R., 2005. „How to buy UV optics”, Opto-Laser Europe, http://optics.org/cws/article/research/21870.